Synthesis of nanostructured TiO_2 thin films with highly enhanced photocatalytic activity by atom beam sputtering

Jaspal Singh[1], Kavita Sahu[1], Sini Kuriakose[1], Nishant Tripathi[2], D. K. Avasthi[3], Satyabrata Mohapatra[1*]

[1]*University School of Basic and Applied Sciences, Guru Gobind Singh Indraprastha University, Dwarka, New Delhi 110078, India*
[2]*Faculty of Engineering and Technology, Jamia Millia Islamia, New Delhi 110078, India*
[3]*Inter University Accelerator Centre, New Delhi 110067, India*

[*]Corresponding author, Tel: (+91) 11 25302414; E-mail: smiuac@gmail.com

Received: 29 March 2016, Revised: 02 August 2016 and Accepted: 03August 2016

DOI: 10.5185/amlett.2017.6432
www.vbripress.com/aml

Abstract

Nanostructured TiO_2 thin films with highly enhanced photocatalytic activity were prepared by atom beam sputtering technique. The effects of thermal annealing on the structural, morphological and photocatalytic properties of TiO_2 thin films were investigated using X-ray diffraction, atomic force microscopy, field emission scanning electron microscopy, Raman spectroscopy and UV-visible absorption spectroscopy. X-ray diffraction studies showed that the as-deposited TiO_2 thin films made up of anatase TiO_2 nanoparticles transformed into anatase/ rutile mixed-phase TiO_2 nanoparticles upon annealing. Field emission scanning electron microscopy and atomic force microscopy studies revealed growth of TiO_2 nanoparticles from 16 nm to 29 nm upon annealing at 600ºC. The photocatalytic activities of the nanostructured TiO_2 thin films were studied by monitoring photocatalytic degradation of methylene blue in water. Our results showed that the as-deposited nanostructured TiO_2 thin films exhibited highly enhanced photocatalytic efficiency as compared to the annealed samples. The mechanism underlying the enhanced photocatalytic activity of nanostructured TiO_2 thin film is tentatively proposed.

Keywords: TiO_2, nanostructures, thin films, sputtering, photocatalysis.

Introduction

Semiconductor photocatalysis has attracted great interest for applications in solar energy conversion and environmental remediation since the discovery of photocatalytic water splitting on TiO_2 in 1972 **[1-3]**. Semiconductors such as ZnO, TiO_2, Fe_2O_3, SnO_2, CuO and Cu_2O act as sensitizers for light-induced redox reactions and lead to photocatalytic degradation of organic contaminants in water and air **[4-8]**. When excited with photons with energy matching or higher than the band gap energy of semiconductor electrons are excited to the conduction band leaving behind holes in the valence band. These photoexcited charge carriers can recombine, dissipate energy as heat, get trapped in surface states or react with electron acceptors and donors adsorbed on the semiconductor surface. The rapid rate of recombination of these charge carriers reduces their participation in redox reactions leading to photocatalytic degradation of organic contaminants and hence limits the photocatalytic activity of semiconductor. Several approaches such as attachment of noble metal nanoparticles **[9-12]**, doping with transition metal **[13]** and coupling of semiconductors **[14,15]** have been employed to suppress the recombination of charge carriers in order to improve the photocatalytic activity. Among the various metal oxide semiconductors TiO_2 is considered as the best photocatalyst because of its excellent optical properties, good chemical stability, low cost and non-toxicity **[16-19]**. Usually nanostructured TiO_2 in powder form is used in diverse photocatalytic applications. However, for advanced photocatalytic applications it is important to develop coatings of TiO_2 nanostructures with enhanced photocatalytic activity on different substrates. Thin film coatings of TiO_2 nanostructures are very promising for photcatalytic degradation of organic pollutants in water and are also attractive for applications in self-cleaning, anti-bacterial and water splitting **[16]**. Therefore, the development of nanostructured TiO_2 coatings with enhanced photocatalytic activity is of immense importance.

Several physical and chemical methods *viz.*, chemical vapor deposition (CVD) **[20, 21]**, solvothermal method **[22, 23]**, sol-gel method **[24]**, pulsed laser deposition (PLD) **[25, 26],** anodic oxidation method **[27, 28],** laser ablation **[29]** and sputtering **[30, 31]** have been employed for the preparation of nanostructured TiO_2 thin films.

In recent years, atom beam sputtering has emerged as a novel and interesting technique to prepare nanostructured thin films and nanocomposites with size controlled nanostructures **[32-43]**. Plasmonic nanocomposites consisting of metal (Au, Ag, Cu) nanoparticles embedded in different matrices including partially oxidized Si, silica, alumina, TiO_2 and ZnO have been synthesized by atom beam sputtering **[32-43]**. In an earlier study, Mishra *et al*. **[33]** reported the synthesis of Ag nanoparticles embedded in silica by the atom beam sputtering and demonstrated its advantages over other ion beam based techniques. Stefanov *et al*. **[44]** reported the preparation of TiO_2 thin films on glass substrates by DC reactive magnetron sputtering and demonstrated their photocatalytic activity towards degradation of 100ppm of methylene blue (MB) dye under UV light in 60 minutes. Dumitriu *et al.* **[45]** prepared TiO_2 thin films on various substrates by DC reactive sputtering and studied their photocatalytic activity through degradation of phenol. Takeda et al. **[46]** prepared TiO_2 thin films by DC magnetron sputtering and studied their photocatalytic activity through decomposition of acetaldehyde. Tavares *et al.* **[47]** prepared polycrystalline TiO_2 thin films by reactive DC sputtering and showed that UV light irradiation leads to photocatalytic degradation of 1 μM Rhodamine B dye in 90 minutes.

In this article, we report synthesis of nanostructured TiO_2 thin films with highly enhanced photocatalytic activity by atom beam sputtering technique. The effects of thermal annealing on the structural, morphological and photocatalytic properties of nanostructured TiO_2 thin films have been investigated. The photocatalytic activity of nanostructured TiO_2 thin films was examined towards sun light driven degradation of MB dye in water. We have demonstrated that the nanostructured TiO_2 thin films prepared by atom beam sputtering exhibit highly enhanced photocatalytic activity, degrading 5 μM MB in 20 minutes upon sun light irradiation. Even though there are few studies, such high photocatalytic activity of nanostructured TiO_2 thin films has not been reported earlier. The mechanism underlying the enhanced photocatalytic activity of atom beam sputtered nanostructured TiO_2 thin film is proposed.

Experimental

Materials

TiO_2 was used as sputtering target, while float zone grown Si(100) was used as substrates. Methylene blue (MB) was purchased from SRL, India. All the chemicals used were of analytical grade and were used as received without any further purification.

Synthesis of nanostructured TiO_2 thin films

Nanostructured TiO_2 thin films were prepared by atom beam sputtering of TiO_2 target with 1.5 keV neutral Ar atoms, using the facility **[27]** at IUAC, New Delhi. The chamber vacuum was $\sim 7 \times 10^{-6}$ mbar while it reached about 1.4×10^{-3} mbar during atom beam sputtering. Thoroughly cleaned Si(100) substrates were used as substrates for deposition of TiO_2 thin films. The sputtered TiO_2 thin film samples were annealed at different temperatures of 400°C and 600°C in Ar atmosphere for 30 minutes. The as-deposited TiO_2 thin film sample and the samples annealed at 400°C and 600°C are here after referred to as S1, S2 and S3, respectively.

Characterizations

The structural properties of the TiO_2 thin films were studied by X-ray diffraction (XRD) using Cu K_α radiation ($\lambda = 0.1542$ nm). The surface morphology of the samples was studied by atomic force microscopy (AFM) using XE-70 Park Systems AFM facility and field emission scanning electron microscopy (FESEM) using FESEM NOVA NANOSEM 450 facility. Raman spectra were recorded by Renishaw Invia Raman microscope equipped with Ar ion laser using a spot size of 1 μm and an excitation wavelength of 514 nm.

Photocatalytic measurements

The photocatalytic activities of the as-deposited and annealed TiO_2 thin films were evaluated by monitoring sun light driven photocatalytic degradation of MB. In a typical experiment, TiO_2 thin film samples were placed inside glass vials containing 5 mL aqueous solutions of 5 μM MB dye and kept in the dark for 60 minutes for allowing adsorption-desorption equilibrium. The solutions with the photocatalyst thin film samples immersed were irradiated with sun light for different durations of time (5, 10 and 20 minutes). After sun light exposure the photocatalyst samples were removed from the solutions and thoroughly washed with double distilled water. The photocatalytic activities of the samples were evaluated by monitoring the change in the absorbance of the characteristic peak of MB at 664 nm using UV-visible absorption spectroscopy. UV-visible absorption spectra of the samples were recorded in the range of 300-800 nm, using a dual beam UV-visible spectrophotometer U3300, with double distilled water as the reference medium. The photocatalytic efficiency of thin films for the photocatalytic degradation of MB dye was calculated with the formula:

$$\eta = (C_0 - C)/ C_0 \quad (1)$$

where, C_0 is the absorbance of MB dye solution before the illumination and C is the absorbance of MB in the solutions after sun light exposure time *t*.

Results and discussion

Morphology and crystal structure

The evolution of surface morphology of TiO_2 thin films upon thermal annealing was studied by AFM. **Fig. 1 (a-c)** shows AFM micrographs of the as-deposited TiO_2 thin film and samples annealed at 400ºC and 600ºC. Figure 1(a) depicts AFM micrograph of as-deposited TiO_2 thin film sample S1 grown on Si substrate. The as-deposited TiO_2 thin film consists of a high density of small nanoparticles. The AFM images of samples annealed at 400ºC and at 600ºC are shown in **Fig. 1(b)** and **(c)**, respectively. It can be clearly seen that annealing resulted

in the growth in size from 15 to 29 nm along with decrease in the number density and aggregation of nanoparticles.

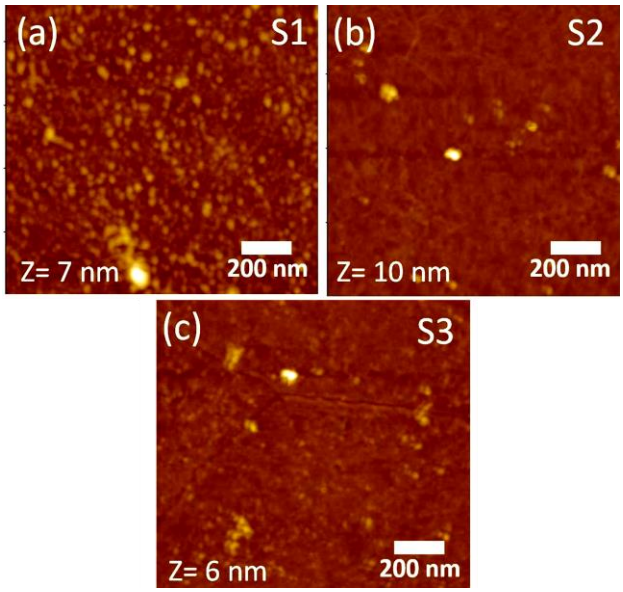

Fig. 1. AFM images of samples (a) S1 (b) S2 and (c) S3.

The dimensions of nanoparticles were extracted using line profiles from AFM images. **Fig. 2(a-c)** shows the FESEM images of the samples S1, S2 and S3. In addition to the growth in size of nanoparticles upon annealing, the presence of aggregates of nanoparticles was also observed in the samples S2 and S3 annealed at 400ºC and 600ºC, respectively. The size distribution histograms of nanoparticles corresponding to the samples S1, S2 and S3 are shown in **Fig. 2(d-f)**. The average size of nanoparticles in the as-deposited sample S1 has been estimated to be 16 nm, while the average nanoparticle size increased to 24 nm for the sample S2 annealed at 400ºC and to 29 nm for the sample S3 annealed at 600ºC. Both AFM and FESEM results clearly show growth of nanoparticles in addition to the formation of nanoparticle aggregates upon annealing.

The structural properties of the samples S1, S2 and S3 were studied by XRD. **Fig. 3(a)** shows the XRD patterns of the samples S1, S2 and S3. In the XRD spectrum of sample S1, peak marked (101) with very low intensity was observed, which clearly shows that the as-deposited thin film is made up of anatase TiO_2 nanoparticles embedded within amorphous TiO_2. Annealing at 400ºC (sample S2) resulted in the formation of nanocrystallites of rutile and anatase TiO_2. This can be clearly seen from the XRD spectrum of S2, which reveals (210) peak closely matching with rutile TiO_2 (JCPDS card No.761940) and (105) peak corresponding to anatase TiO_2 (JCPDS card No.211272).

For the sample S3, the diffraction pattern shows peaks (101), (200) and (105) corresponding to the anatase phase of TiO_2 (JCPDS card No.211272). It can be seen that annealing at 600ºC led to the emergence of a stronger (101) peak characteristic of anatase TiO_2 indicating the transformation of the nanostructured TiO_2 thin film into a sample with larger fraction of anatase TiO_2.

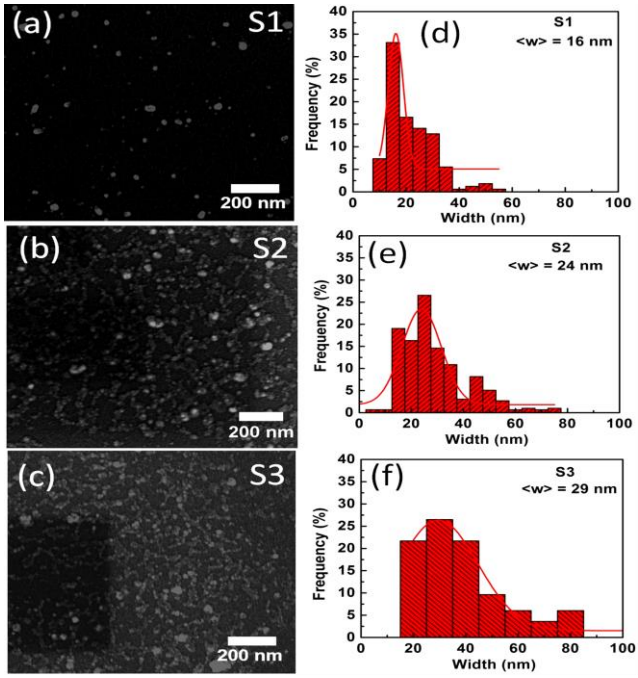

Fig. 2. (a-c) FESEM images of samples S1, S2 and S3. (d-f) corresponding size distributions of nanostructures in the samples S1, S2 and S3.

In an earlier study, Mohanty *et al.* **[48]** reported the structural transformation of TiO_2 thin films under different oxygen partial pressure and showed that anatase TiO_2 is formed from rutile phase with an increase in partial pressure.

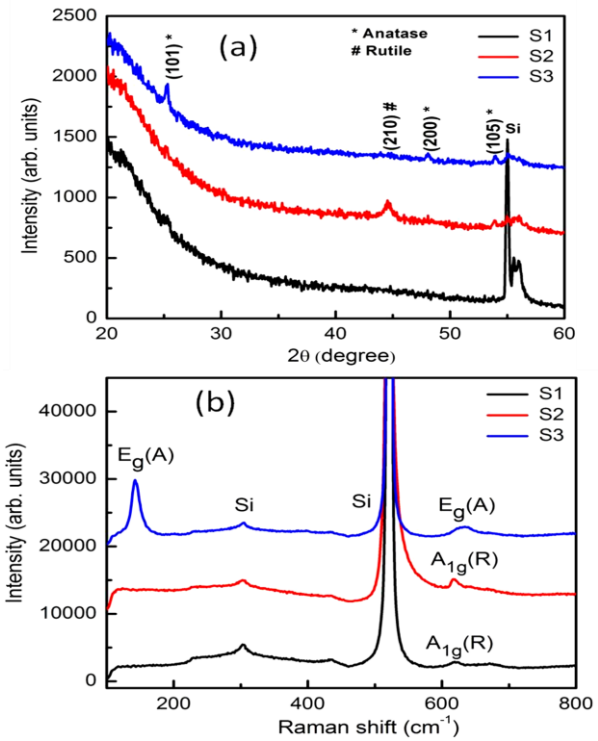

Fig. 3. (a) XRD patterns of samples S1, S2 and S3, (b) Raman spectra of samples S1, S2 and S3.

Raman spectroscopy was used to study thermal annealing induced structural transformation of TiO_2

nanostructures in the atom beam sputtered TiO_2 thin films. TiO_2 with anatase phase belongs to the space group D^{19}_{4h} **[49]** and has six Raman active modes ($1A_{1g} + 2B_{1g} + 3E_g$) **[50]**. Anatase TiO_2 exhibits six Raman active modes at 144 cm^{-1} (E_g), 197 cm^{-1} (E_g), 399 cm^{-1} (B_{1g}), 516 cm^{-1} ($A_{1g} + B_{1g}$), and 639 cm^{-1} (E_g) **[51]**. **Fig. 3(b)** shows the Raman spectra of the as-deposited TiO_2 thin film sample S1 and annealed samples S2 and S3. In all the samples the observed peaks at ~ 303 cm^{-1} and 520 cm^{-1} originate from the Si substrate used for deposition of thin films and correspond to the longitudinal acoustic (LA) mode of a-Si and asymmetric transverse optical mode of c-Si, respectively **[52]**. For the sample S1, the presence of a very small peak at 617 cm^{-1} indicates the presence of small content of rutile TiO_2 nanoparticles within the amorphous TiO_2 film, as seen from our XRD results. The observed peak at 617 cm^{-1} corresponds to the A_{1g} mode of rutile TiO_2, which increased in intensity upon annealing at 400°C (sample S2). As the annealing temperature is further increased to 600°C (sample S3), the Raman spectrum reveals distinct peaks at 145 cm^{-1} and 634 cm^{-1} corresponding to the E_g and E_g modes of anatase TiO_2, respectively **[53]**.

The formation and growth mechanism of TiO_2 nanoparticles in the as-deposited thin film prepared by atom beam sputtering is schematically depicted in **Fig. 4** and can be understood as follows. Irradiation of TiO_2 with 1.5 keV Ar atoms leads to the sputtering of Ti and O atoms with energies of the order of few eV to hundreds of eV, as estimated using the SRIM program **[54]**. These energetic sputtered Ti and O atoms get deposited on the Si substrate. The formation of TiO_2 nanoparticles in the deposited thin film involves processes such as surface and bulk diffusion of deposited O and Ti atoms leading to nucleation and growth of TiO_2 nanoclusters and adsorption/ desorption of atoms from the TiO_2 nanoclusters on surface of the TiO_2 thin film growing on the Si substrate. The energy of the sputtered Ti and O atoms deposited in the film facilitates the growth of TiO_2 nanostructures leading to the growth of nanostructured TiO_2 thin film.

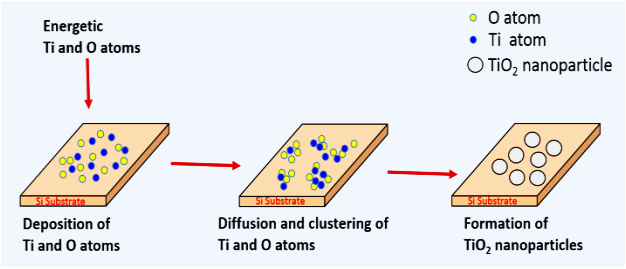

Fig. 4. Growth mechanism of TiO_2 nanostructures on Si substrate by atom beam sputtering method.

Photocatalytic studies

The photocatalytic activities of as-deposited and annealed nanostructured TiO_2 thin films were evaluated by monitoring sun light driven photocatalytic degradation of MB in water. **Fig. 5 (a-c)** shows the UV-visible absorption spectra of 5 μM MB aqueous solutions with the as-deposited and annealed TiO_2 thin films upon sun light irradiation for different durations. The intensity of the characteristic peak of MB at 664 nm was monitored and was found to drastically decrease with increase in the sun light irradiation time in all the three samples. From the optical absorption spectra it can be clearly seen that the sample S1 exhibits the highest photocatalytic efficiency for photocatalytic degradation of MB as compared to the samples S2 and S3. **Fig. 5(d)** shows the kinetics of photocatalytic degradation of MB by using samples S1, S2 and S3 under sun light exposure. It can be seen that following 20 minutes of sun light exposure the samples S2 and S3 led to degradation of 61% and 84% of MB dye, respectively, whereas the sample S1 exhibited the highest photocatalytic efficiency of 95% for the same irradiation time.

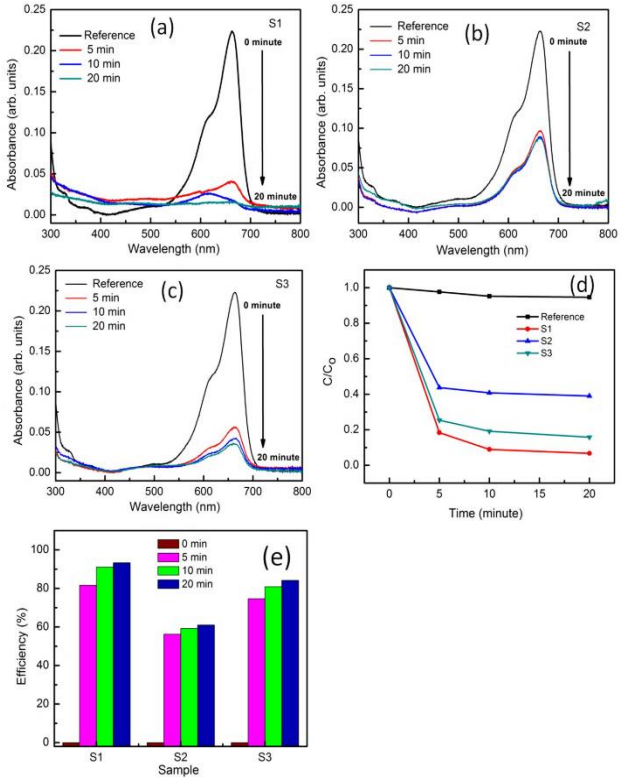

Fig. 5. (a-c) UV-visible absorption spectra showing sun light driven photocatalytic degradation of MB in water using samples S1, S2 and S3 as photocatalysts, (d) Kinetics of photocatalytic degradation of MB in water using samples S1, S2, and S3 as photocatalysts, (e) Variation of photocatalytic efficiency of samples S1, S2 and S3 for the photocatalytic degradation of MB dye in water.

The photocatalytic degradation of MB dye in water by nanostructured TiO_2 thin films follows first-order kinetics and the rate constants were calculated using the formula given by

$$C = C_0 \exp(-kt) \quad (2)$$

where, k is the first-order rate constant. The rate constants (k) have been calculated by linear fitting to the $\ln(C/C_o)$ versus time plots. For the samples S1, S2 and S3 the values of k are found to be 0.162 min^{-1}, 0.06 min^{-1} and 0.114 min^{-1}, respectively. The photocatalytic efficiency of the samples towards photocatalytic degradation of MB

was found to follow an order S1 > S3 > S2, which can also be clearly seen from the **Fig. 5(e)**. It can be clearly seen that the atom beam sputtered nanostructured TiO_2 thin films exhibit very strong photocatalytic activity for degradation of MB in water, which opens up possibilities for promising practical applications of these advanced photocatalytic coatings.

The mechanisms involving the charge transportation processes underlying the highly enhanced photocatalytic activity of nanostructured TiO_2 thin films towards photocatalytic degradation of MB dye are depicted in **Fig. 6**.

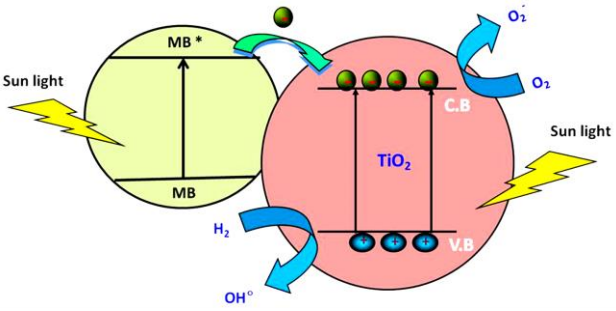

Fig. 6. Schematic diagram showing underlying charge transfer processes leading to photocatalytic degradation of dye.

The first step involves the adsorption of MB dye molecules on to the surface of nanostructured TiO_2 thin films. When TiO_2 thin film samples with MB dye molecules adsorbed on their surfaces are exposed to sunlight, TiO_2 nanostructures absorb photons leading to the generation of photoexcited electrons in the conduction band and holes in the valance band of TiO_2 (Eq. 3). In addition, the MB dye molecules get excited by sun light resulting in the transfer of electrons into the conduction band of TiO_2. The electrons in the conduction band of TiO_2 react with oxygen molecules present at the surface and form super oxide radicals ($O_2^{\bullet -}$) (Eq. 4). The holes generated in the valance band interact with water molecules to form hydroxyl radicals ($OH^{\bullet}$) (Eq. 5). Some of the super oxide radicals react with H^+ to form $HO_2^{\bullet}$, which get converted to hydrogen peroxide (H_2O_2) (Eq. 7), which leads to an enhancement in the photocatalytic activity. The highly reactive super oxide and hydroxyl radicals interact with the MB dye molecules adsorbed on the surface of nanostructured TiO_2 thin films and lead to their photocatalytic degradation involving the following reactions **[55]**.

$$TiO_2 + hv \rightarrow e_{CB}^- + h_{VB}^+ \quad (3)$$

$$(O_2)_{ads} + e_{CB}^- \rightarrow O_2^{\cdot -} \quad (4)$$

$$(H_2O)_{ads} + h_{VB}^+ \rightarrow H^+ + OH^{\cdot} \quad (5)$$

$$O_2^{\cdot -} + H^+ \rightarrow HO_2^{\cdot} \quad (6)$$

$$2HO_2^{\cdot} \rightarrow H_2O_2 + O_2 \quad (7)$$

$$OH^{\cdot} + Organic\ dye \rightarrow degradation\ product \quad (8)$$

$$O_2^{\cdot -} + Organic\ dye \rightarrow degradation\ product \quad (9)$$

Photocatalytic efficiency of nanostructured TiO_2 thin films is strongly dependent on the size, surface area and crystal structure of the TiO_2 nanostructures. Results of our photocatalytic studies show that the as-deposited nanostructured TiO_2 thin film sample exhibits the highest photocatalytic activity for sun light driven photocatalytic degradation of MB in water. Sample S1 contains anatase TiO_2 nanoparticles with smallest average size of 15 nm, which provide a relatively higher surface area for adsorption of MB dye molecules leading to the enhanced photocatalytic activity. Thermal annealing leads to growth in size of TiO_2 nanoparticles and significant change in the crystal structure of nanostructured TiO_2 thin films, both of which affect the photocatalytic activity. Sample S2 annealed at 400°C contains TiO_2 nanoparticles with larger average size as compared to the sample S1. Moreover, it is clear from our Raman spectroscopy and XRD results that the sample S2 contains rutile TiO_2 nanostructures, which is not favorable for achieving enhanced photocatalytic activity **[56]**. The nanostructured TiO_2 sample S3 annealed at 600°C contains larger aggregates of TiO_2 nanoparticles with anatase phase, which result in improved photocatalytic activity **[57]**. Due to this the sample S3 exhibits stronger photocatalytic activity towards degradation of MB as compared to the sample S2. We have demonstrated that nanostructured TiO_2 thin film prepared by atom beam sputtering leads to highly efficient photocatalytic activity towards photocatalytic degradation of MB dye in water, which is promising for developing advanced photocatalytic coatings for practical applications in environmental remediation.

Conclusion

In summary, we have synthesized nanostructured TiO_2 thin films with highly enhanced photocatalytic activity by atom beam sputtering technique. The effects of thermal annealing on the structural, morphological and photocatalytic properties of nanostructured TiO_2 thin films have been investigated. The as-deposited nanostructured TiO_2 thin film prepared by atom beam sputtering exhibits highly enhanced photocatalytic activity towards sun light driven photocatalytic degradation of MB dye in water, as compared to the annealed samples. The enhanced photocatalytic activity of as-deposited nanostructured TiO_2 thin film prepared by atom beam sputtering is attributed to the combined effects of anatase phase and smaller size of TiO_2 nanoparticles providing higher surface area for enhanced dye adsorption and efficient photocatalytic degradation upon sun light irradiation. The nanostructured TiO_2 thin films lead to almost complete degradation of MB dye in water in only 20 minutes and are very promising for use in advanced photocatalytic coatings for practical applications environmental remediation.

Acknowledgements

The authors are thankful to Deepty and S. R. Abhilash for their help in sample preparation, Mohit for XRD measurements, Dr. F. Singh for Raman measurements and Dr. T. Som for extending the XRD facility. SM is thankful to Department of Science and Technology (DST), New Delhi for providing AFM facility at Guru Gobind Singh Indraprastha University, New Delhi under Nano Mission (SR/NM/PG-17/2007). SM gratefully acknowledges funding from DST, New Delhi for Micro-Raman and UV-visible-NIR spectrophotometer facilities at Guru Gobind Singh Indraprastha University, New Delhi under FIST

program (SR/FST/PSI-167/2011(C)). JS is thankful to University Grants Commission (UGC), New Delhi for providing financial assistance through Maulana Azad National Fellowship.

Author contributions

Conceived the plan: SM; Performed the experiments: JS, KS, SK, NT, SM; Data analysis: JS; Wrote the paper: JS, DKA, SM (JS, KS, SK, NT, DKA, SM are the initials of authors). Authors have no competing financial interests.

References

1. Fujishma, A.; Honda, K. *Nature* **1972**, *238*, 37. **DOI:**10.1038/238037a0
2. Linsebigler, L.; Lu, G.; and Yates, J. T. *Chem. Rev.* **1995**, *95*, 735. **DOI:** 10.1021/cr00035a013
3. Schneider, J.; Matsuoka, M.; Takeuchi, M.; Zhang, J.; Horiuchi, Y.; Anpo, M.; and Bahnemann, D. W. *Chem. Rev*. **2014**, *114*, 9919. **DOI:** 10.1021/cr5001892
4. Kuriakose, S.; Bhardwaj, N.; Singh, J.; Satpati, B.; and Mohapatra, S. *Beilstein J. Nanotechnol.* **2013**, *4*, 763. **DOI:** 10.3762/bjnano.4.87
5. Cao,Y.; Zhang,X.; Yang,W.; Du, H.; Bai, H.; Li, H.; and Yao. J.; *Chem. Mater.* **2000**, *12*, 3445. **DOI:**10.1021/cm0004432.
6. Shukla, S. K.; Bharadvaja, A.; Parashar, G. K.; Mishra, A. P.; Dubey, G. C.; Tiwari, A.; *Advanced Materials Letters*, **2012**, 3, 365. **DOI:** 10.5185/amlett.2012.5350
7. Reimer, T.; Paulowicz, I.; Röder, R.; Kaps, S.; Lupan, O.; Chemnitz, S.; Benecke, W.; Ronning, C.; Adelung, R.; and Mishra, Y. K.; *ACS Appl. Mater. Interfaces* **2014**, *6*, 7806. **DOI:** 10.1021/am5010877
8. Mishra, Y.K.; Modi, G.; Cretu, V.; Postica,V.; Lupan, O.; Reimer, T.; Paulowicz, I.; Hrkac, V.; Benecke, W.; Kienle, L.; and Adelung, R.; *ACS Appl. Mater. Interfaces* **2015**, *7*, 14303−14316. **DOI:** 10.1021/acsami.5b02816
9. Kuriakose, S.; Choudhary,V.; Satpati, B.; and Mohapatra, S. *Beilstein J. Nanotechnol.* **2014**, *5*, 639. **DOI:** 10.3762/bjnano.5.75
10. Kuriakose, S.; Choudhary,V.; Satpati, B.; and Mohapatra, S. *Phys. Chem. Chem. Phys.* **2014**, *16*, 17560. **DOI:** 10.1039/c4cp02228a
11. Kuriakose, S.; Satpati, B.; and Mohapatra, S. *Phys. Chem. Chem. Phys.* **2015**, *17*, 25172. **DOI:** 10.1039/C5CP01681A
12. Peralta, M.D. L. R.; Pal, U.; and Zeferino, R. S.; *ACS Appl. Mater. Interfaces* **2012**, *4*, 4807. **DOI:** 10.1021/am301155u
13. Kuriakose, S.; Satpati, B.; and Mohapatra, S. *Phys. Chem. Chem. Phys.* **2014**, *16*, 12741. **DOI:** 10.1039/c4cp01315h
14. Kuriakose, S.; Avasthi,D.K.; and Mohapatra, S. *Beilstein J. Nanotechnol.* **2015**, *5*, 928. **DOI:** 10.3762/bjnano.6.96
15. Pawar, R.C.; Lee, C. S.; *Appl. Catal. B: Environ.* **2014**, *144*, 57. **DOI:** 10.1016/j.apcatb.2013.06.022
16. Hoshimoto, K.; Irie, H.; Fujishima, A. *Jap. J. Appl. Phys*. **2005**, *44*, 8269. **DOI:**10.1143/JJAP.44.8269
17. Chen, X.; and Mao, S. S. *Chem. Rev*. **2007**, *107*, 2891. **DOI:**10.1021/cr0500535
18. Kubacka, A.; García, M. F.; and Colon, G. *Chem. Rev*. **2012**, *112*, 1555. **DOI:** 10.1021/cr100454n
19. Ni, M.; Leung, M. K. H.; Leung, D. Y. C.; Sumathy, K. *Renew. Sustain. Energy Rev*. **2007**, *11*, 401. **DOI:** 10.1016/j.rser.2005.01.009
20. Borras, A.; Sanchez-Valencia, J. R.; Widmer, R.; Rico, V. J.; Justo, A.; and Gonzalez-Elipe, A. R. *Cryst. Growth Design*. **2009**, *9*, 2868. **DOI:** 10.1021/cg9001779
21. Hyett, G.; Green, M.; and Parkin, I. P. *J. Am. Chem. Soc.* **2006**, *128*, 12147-12155. **DOI:** 10.1021/ja062766q
22. Yang, H. G.; Liu, G.; Qiao, S. Z.; Sun, C. H.; Jin, Y. G.; Smith, S. C.; Zou, J.; Cheng, H. M.; and Lu, G. Q. *J. Am. Chem. Soc*. **2009**, *131*, 4078. **DOI:** 10.1021/ja808790p
23. Lan, C. M.; Liu, S. E.; Shiu, J. W.; Hu, J. Y.; Lin, M. H.; Diau, E. W. G. *RSC Adv.* **2013**, *3*, 559. **DOI:** 10.1039/C2RA22807F
24. Singh, J.; Mohapatra, S. *Adv. Mater. Lett.* **2015**, *6*, 924. **DOI:** 10.5185/amlett.2015.6000
25. Gyorgy, E.; Socol, G.; Axente, E.; Mihailescu, I. N.; Ducu, C.; Ciuca, S. *Appl. Surf. Sci.* **2005**, *247*, 429. **DOI:** 10.1016/j.apsusc.2005.01.074
26. Suda, Y.; Kawasaki, H.; Ueda, T.; Ohshima, T. *Thin Solid Films* **2004**, *453*, 162. **DOI:** 10.1016/j.tsf.2003.11.185
27. Xu, X.; Tang, C.; Zeng, H.; Zhai, T.; Zhang, S.; Zhao, H.; Bando, Y.; and Golberg, D.; *ACS Appl. Mater. Interfaces* **2011**, *3*, 1352. **DOI:** 10.1021/am200152b
28. Xu, X.; Fang, X.; Zhai, T.; Zeng, H.; Liu, B.; Hu, X.; Bando,Y.; and Golberg, D.; *Small* **2011**, *7*, 445. **DOI:** 10.1002/smll.201001849
29. Liu, P.; Cai1, W.; Fang, M.; Li, Z.; Zeng, H.; Hu, J.; Luo, X.; and Jing, W.; *Nanotechnology* **2009**, *20*, 285707. **DOI:** 10.1088/0957-4484/20/28/285707
30. Kitano, M.; Funatsu, K.; Matsuoka, M.; Ueshima, M.; and Anpo, M. *J. Phys. Chem. B* **2006**, *110*, 25266. **DOI:** 10.1021/jp064893e
31. Tanemura, S.; Miao, L.; Wunderlich, W.; Tanemura, M.; Mori, Y.; Toh, S.; Kaneko, K. *Sci. Technol. Adv. Mater*. **2005**, *6*, 11. **DOI:** 10.1016/j.stam.2004.06.002
32. Kabiraj, D.; Abhilash, S. R.; Vanmarcke, L.; Cinausero, N.; Pivin, J. C.; Avasthi, D. K. *Nucl. Instrum. Meth. B.* **2006**, *244*, 100. **DOI:** 10.1016/j.nimb.2005.11.018
33. Mishra, Y. K.; Mohapatra, S.; Kabiraj, D.; Mohanta, B.; Lalla, N. P.; Pivin, J. C.; Avasthi, D. K. *Scripta Mater.* **2007**, *56*, 629. **DOI:** 10.1016/j.scriptamat.2006.12.008
34. Mishra, Y. K.; Mohapatra, S.; Avasthi, D. K.; Kabiraj, D.; Lalla, N. P.; Pivin, J. C.; Sharma, H.; Kar, R.; Singh, N. *Nanotechnology* **2007**, *18*, 345606. **DOI:** 10.1088/0957-4484/18/34/345606
35. Mohapatra, S.; Mishra, Y. K.; Avasthi, D. K.; Kabiraj, D.; Ghatak, J.; Varma, S. *J. Phys. D: Appl. Phys.* **2007**, *40*, 7063. **DOI:**10.1088/0022-3727/40/22/030
36. Mohapatra, S.; Mishra, Y. K.; Ghatak, J.; Kabiraj, D.; and Avasthi, D. K. *J. Nanosci. Nanotechnol.* **2008**, *8*, 4285. **DOI:** 10.1166/jnn.2008.AN30
37. Mohapatra, S.; Mishra, Y. K.; Avasthi, D. K.; Kabiraj, D.; Ghatak, J.; Varma, S. *Appl. Phys. Lett.* **2008**, *92*, 103105. **DOI:** 10.1063/1.2894187
38. Mishra, Y. K.; Mohapatra, S.; Singhal, R.; Agarwal, D. C.; Avasthi, D. K.; Ogale, S. B. *Appl. Phys. Lett.* **2008**, *92*, 043107. **DOI:** 10.1063/1.2838302
39. Tiwary, M.; Agarwal, D. C.; Mohapatra, S.; Pivin, J. C.; Avasthi, D. K.; Annapoorni, S. *Physica Status Solidi A* **2012**, *209*, 2499. **DOI:** 10.1002/pssa.201228362
40. Mohapatra, S.; Mishra, Y. K.; Warrier, A. M.; Philip, R.; Sahoo, S.; Arora, A. K.; Avasthi, D. K. *Plasmonics* **2012**, *7*, 25. **DOI:** 10.1007/s11468-011-9271-y
41. Kumar, M.; Kumar, T.; Avasthi, D. K. *Scripta Mater*. **2015**, *105*, 46. **DOI:** 10.1016/j.scriptamat.2015.04.030
42. Avasthi, D. K.; Mishra, Y. K.; Kabiraj, D.; Lalla, N. P.; and Pivin, J.C. *Nanotechnology* **2007**, *18*, 125604. **DOI:** 10.1088/0957-4484/18/12/125604
43. Mohapatra, S. *Phys. Chem. Chem. Phys.* **2016**, *18*, 3878. **DOI:** 10.1039/C5CP05345E
44. Stefanov, B.; and Österlund, L. *Coatings* **2014**, *4*, 587. **DOI:** 10.3390/coatings4030587
45. Dumitriu, D.; Bally, A. R.; Ballif, C.; Hones, P.; Schmid, P. E.; Sanjinés, R.; Lévy, F.; Pârvulescu, V. I. *Appl. Catal. B: Environ.* **2000**, *25*, 83. **DOI:** 10.1016/S0926-3373(99)00123-X
46. Takeda, S.; Suzuki, S.; Odaka, H.; Hosono, H.; *Thin Solid Films* **2001**, *392*, 338. **DOI:** 10.1016/S0040-6090(01)01054-9

47. Tavares, C. J.; Vieira, J.; Rebouta, L.; Hungerford, G.; Coutinho, P.; Teixeira, V.; Carneiro, J. O.; Fernandes, A. J. *Mater. Sci. Eng. B* **2007**, *138*, 139. **DOI:** 10.1016/j.mseb.2005.11.043
48. Mohanty, P.; Mishra, N. C; Choudhary, R. J.; Banerjee, A.; Shripathi, T.; Lalla, N. P.; Annapoorni, S.; Rath, C. *J. Phys. D: Appl. Phys.* **2012**, *45*, 325301. **DOI:**10.1088/0022-3727/45/32/325301
49. Chen, C. A.; Huang, Y. S.; Chung, W. H.; Tsai, D. S.; Tiong, K. K. *J. Mater. Sci.* **2009**, *20*, S303. **DOI:** 10.1007%2Fs10854-008-9595-3
50. Loudon, R. *Adv. Phys.* **1964**, *13*, 423. **DOI:** 10.1080/00018736400101051
51. Ohsaka, T.; Izumi, F.; Fujiki, Y. *J. Raman Spectrosc.* **1978**, *7*, 321. **DOI:** 10.1002/jrs.1250070606
52. Wen, C.; Xu, H.; Liu, H.; Li Z.; and Shen, W. *Nanotechnology* **2013**, *24*, 455602. **DOI:** 10.1088/0957-4484/24/45/455602
53. Yin, H.; Wada, Y.; Kitamura, T.; Kambe, S.; Murasawa, S.; Mori, H.; Sakata, T.; and Yanagida, S. *J. Mater. Chem.* **2001**, *11*, 1694. **DOI:** 10.1039/B008974P
54. Ziegler, J. F.; Biersack, J. P.; Littmark, U. *Stopping Power and Ranges of Ion in Matter*, Pergamon, New York, **1985**.
55. Tang, W. Z.; An, H. *Chemosphere* **1995**, *31*, 4171. **DOI:** 10.1016/0045-6535(95)80016-E
56. Luttrell, T.; Halpegamage, S.; Tao, J.; Kramer, A.; Sutter, E.; and Batzill, M. *Sci. Rep.* **2014**, *4*, 4043. **DOI:** 10.1038/srep04043
57. Yang, H. G.; Liu, G.; Qiao, S. Z.; Sun, C. H.; Jin, Y. G.; Zou, Z.; Smith, S. C.; Cheng, H. M.; Lu, G. Q. *J. Am. Chem. Soc.* **2009**, *131*, 4078. **DOI:** 10.1021/ja808790p